Comparison. The scaphoid of *R. velaunum* shows many similarities with that of *R. romani*: the anterior and posterior heights are equal, the proximal articulation for the radius is triangular, the anterodistal facet for the magnum is very concave and the facet for the trapezoid is extended anteriorly. However, it differs by a smaller size, a better development of the trapezium facet and a less well developed tuberosity below the proximal articulation. The scaphoid of *R. filholi* is also similar to the scaphoid of *R. romani*, especially in its development of the distolateral apophysis (bearing the magnum facet). The scaphoid from Quercy attributed to ?*R. filholi* is almost identical, and also shows the typical fusion of the anteroproximal and postero-proximal facets for the lunate. The scaphoids of *Diaceratherium asphaltense* (Depéret & Douxami, 1902) from Pyrimont (FSL213008), *D. lamilloquense* (Michel 1983; Duranthon 1990), *D. aginense* from Laugnac (MHNM.1996.17.94) and *D. aurelianense* (Nouel, 1866) from Neuville-aux-Bois (MHNB41.2018.0.282, -.384 and -.866) differ from *R. romani* by a higher posterior height compared to the anterior, a more convex dorsal border in proximal view, a flattened articulation for the magnum, a much more concave articulation for the trapezoid and a larger articulation for the trapezium. Furthermore, *D. aurelianense* also greatly differs by the deep and wide groove separating the anteroproximal and postero-proximal facets for the lunate, as in *Pleuroceros blanfordi* (Antoine *et al*. 2010: fig. 6) or *Teleoceras aepysoma* (Short *et al*. 2019: fig. 45), whereas in *Ronzotherium* they are either completely fused or partly connected, although in *D. lamilloquense* from La Milloque and Castelmaurou they also seem to be fused (Michel 1983; Duranthon 1990). In *D. asphaltense*, this postero-proximal facet seems absent.

Lunate. It is only known from Rickenbach (NMO-I7/115 and NMB-Ri-27, Fig. 21H). One is complete (NMO-I7/115) but the other is broken. The proximal articulation for the radius is large and convex anteroposteriorly. It occupies the whole anteroproximal border, there is no articulation with the ulna. In proximal view, there is a drop-like posterior extension of the radius facet on the medial border. In anterior view, the proximal border is much wider than the distal part. The anterior side is deeply keeled. There are two medial articulations, two lateral and two distal. In lateral view, there is only one proximal articulation facet for the scaphoid, which occupies the whole proximal border, formed by the fusion of the anteroproximal and postero-proximal facets, as on the scaphoid. A shallow groove separates the proximal facet from the distal one. This distal facet for the scaphoid is high, almost triangular and restricted to the anterior portion of the lunate. In medial view, the proximal and distal articulations for the pyramidal are rather small, but they are not in the same plane, the proximal one is more medially displaced. The proximal one is a half oval, whereas the distal one is band-shaped and posteriorly displaced. In distal view, there are two large articulation facets: an anterior one for the unciform, and a distal one for the magnum, very concave, with a thin band-shaped anterior elongation separating the

Fig. 18 (next page). *Ronzotherium romani* Kretzoi, 1940 from St-Henri/St-André/Les-Milles, near Marseille (late Oligocene, France). – **A**. Left scaphoid FSL-520285. **A1**. Medial view. **A2**. Lateral view. **A3**. Proximal view. **A4**. Distal view. – **B**. Right trapezoid FSL-9501. **B1**. Anterior view. **B2**. Lateral view. **B3**. Medial view. **B4**. Proximal view. **B5**. Distal view. – **C**. Right unciform NMB-Mar-865. **C1**. Anterior view. **C2**. Medial view. **C3**. Lateral view. **C4**. Proximal view. **C5**. Distal view. – **D**. Left McIV FSL-520287. **D1**. Proximal view. **D2**. Anterior view. **D3**. Medial view. **D4**. Lateral view. – **E**. Right distal femur NMB-Mar-828. **E1**. Anterior view. **E2**. Distal view. – **F**. Right navicular NMB-Mar-847e. **F1**. Lateral view. **F2**. Proximal view. **F3**. Distal view. – **G**. Right cuboid NMB-Mar-847d. **G1**. Anterior view. **G2**. Proximal view. **G3**. Distal view. **G4**. Medial view. **G5**. Lateral view. – **H**. Left ectocuneiform NMB-Mar-735. **H1**. Proximal view. **H2**. Anterior view. **H3**. Lateral view. **H4**. Medial view. – **I**. Right MtII NMB-Mar-847a. **I1**. Anterior view. **I2**. Lateral view. – **J**. Left MtIV FSL-520286. **J1**. Proximal view. **J2**. Anterior view. **J3**. Medial view. Abbreviations: a = astragal; adl = anterodistal facet for the lunate; apl = anteroproximal facet for the lunate; c = cuboid; ca = calcaneus; ec = ectocuneiform; en = entocuneiform; l = lunate; m = magnum; mc = mesocuneiform; n = navicular; p = pyramidal; ppl = postero-proximal facet for the lunate; r = radius; s = scaphoid; td = trapezoid; tm = trapezium; un = unciform. Scale bar: 2 cm.

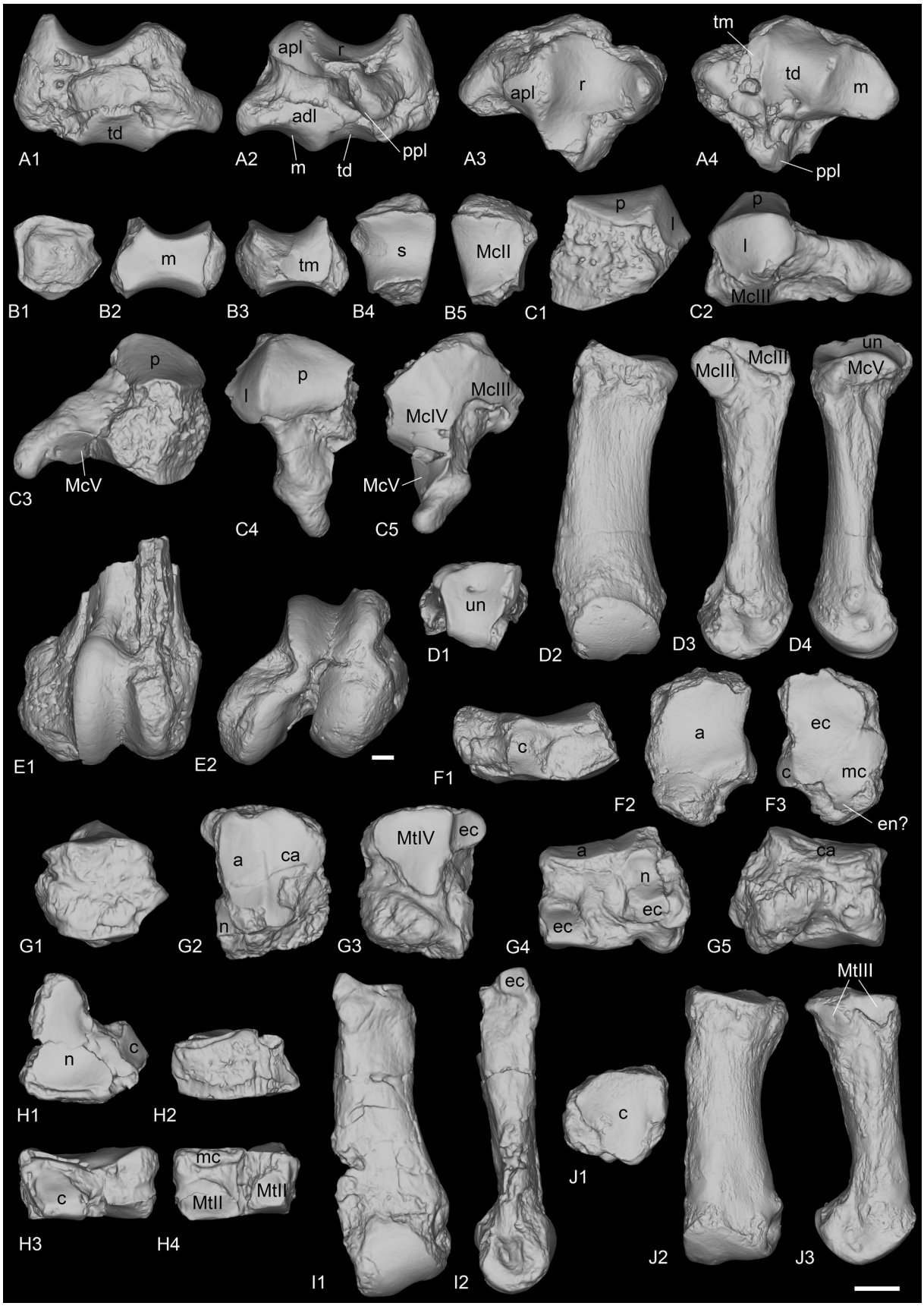
A1
td
A2
apl
r
adl
m
td
ppl
A3
apl
r
A4
tm
td
m
ppl
B1
B2
m
B3
tm
B4
s
B5
McII
C1
p
l
C2
p
l
McIII
C3
p
McV
C4
p
l
C5
McIII
McIV
McV
D1
un
D2
D3
McIII
McIII
D4
un
McV
E1
E2
F1
c
F2
a
F3
ec
c
mc
en?
G1
G2
a
ca
n
G3
MtIV
ec
G4
a
n
ec
ec
G5
ca
H1
n
c
H2
H3
c
H4
mc
MtII
MtII
I1
I2
ec
J1
c
J2
J3
MtIII

scaphoid facet from the unciform facet. The unciform facet occupies almost all of the distal border of the bone in anterior view and is nearly horizontal. The magnum facet is very small in anterior view and makes a very weak angle with the distal scaphoid facet.

Comparison. Although the lunate of *R. velaunum* from Ronzon is not fully extracted from the sediment, the visible part of the bone is similar to the lunate from Rickenbach. The proximal articulation for the radius is very wide and has a posterior extension. The posterior tuberosity is larger and wider than in Rickenbach. On the medial side, the two facets for the pyramidal are not in the same plane either, though on the specimen from Ronzon, the distal facet is much larger. These characters are also found in the lunate of *R. filholi* from Villebramar (Brunet 1979). However, the lunates of *R. velaunum* and *R. filholi* (both from Villebramar and Quercy) differ by the presence of a shallow groove separating the anteroproximal facet for the scaphoid from the postero-proximal one. The lunates of *Diaceratherium tomerdingense* (SMNS-16157c), *D. aurelianense* (Cerdeño 1993), *D. aginense* (MHNM.1996.17.21) and *D. asphaltense* (FSL-213008) differ by their reduced posterior tuberosity in proximal view, the reduced or absent posterior extension of the proximal facet for the radius and the much more proximo-distally compressed anterior side. They also mostly differ by the wide groove separating the anteroproximal facet for the scaphoid from the postero-proximal one as well as the larger anterior portion of the facet for the magnum (it is almost as large as the distal pyramidal facet). In *D. lamilloquense* from Castelmaurou (TLM.PAL.2014.0.2571), this postero-proximal facet for the scaphoid is either absent or separated from the anterior by a large groove, as in other diaceratheres, and the magnum facet is also rather large anteriorly. On the preserved hand of *D. lemanense* from Gannat (MNHN-LIM-598), the anterior portion of the magnum facet is also very large, as in other diaceratheres but the scaphoid facets are not visible.

Pyramidal. It is only known from Rickenbach (NMO-I11-82, Fig. 21I) and almost complete. The proximal ulna facet is large, saddle-shaped, concave anteroposteriorly, transversally convex and medially elongated. It contacts the long band-shaped postero-proximal pisiform facet. There are two lateral facets for the lunate: the proximal one is half-oval, and the distal one is asymmetrical. They are separated by a wide and shallow groove, and are not exactly in the same plane, in the same way as the two corresponding facets on the lunate. Furthermore, their size, shape and position also fit with it. The distal articulation for the unciform is triangular in distal view and concave anteroposteriorly.

Comparison. This specimen is almost identical to the pyramidal of *R. velaunum* MNHN.F.RZN.502, both in size and morphology. It only differs by a larger distal facet for the lunate, and a deeper groove between the two facets for the lunate. The pyramidal of *R. filholi* is overall also very similar but shows a deeper groove between the two lunate facets, as well as a tubercle on the posterior side, below the unciform facet, which is absent in *R. romani*. The pyramidals of *D. tomerdingense* (SMNS-16157d) and *D. aginense* (MHNM.1996.17.20) differ however by very different proportions: the anterior side is lower and more anteroposteriorly elongated, and the medial side, corresponding to the lunate, is extremely reduced proximo-dorsally. They also differ by their less elongated and drop-shaped facet for

Fig. 19 (next page). *Ronzotherium romani* Kretzoi, 1940 from Gaimersheim (late Oligocene, Germany). – **A–D**. Right radius. **A**. Anterior view. **B**. Disto-lateral view. **C**. Distal view. **D**. Proximal view. – **E–H**. Right scaphoid. **E**. Medial view. **F**. Lateral view. **G**. Proximal view. **H**. Distal view. – **I–L**. Left magnum. **I**. Anterior view. **J**. Lateral view. **K**. Medial view. **L**. Distal view. – **M, P–R, U**. Right McIII. **M**. Anterior view. **P**. Posterior view. **Q**. Proximo-medial view. **R**. Proximo-lateral view. **U**. Proximal view. – **N–O, S–T, V**. Right McIV. **N**. Anterior view. **O**. Posterior view. **S**. Proximo-lateral view. **T**. Proximo-medial view. **V**. Proximal view. Abbreviations: adl = anterodistal facet for the lunate; apl = anteroproximal facet for the lunate; h = humerus; im = insertion for the m. biceps brachii; l = lunate; m = magnum; ppl = postero-proximal facet for the lunate; pt = posterior tuberosity; r = radius; s = scaphoid; td = trapezoid; tm = trapezium; u = ulna; un = unciform. All specimens from BSPG collection. Scale bars: 2 cm.

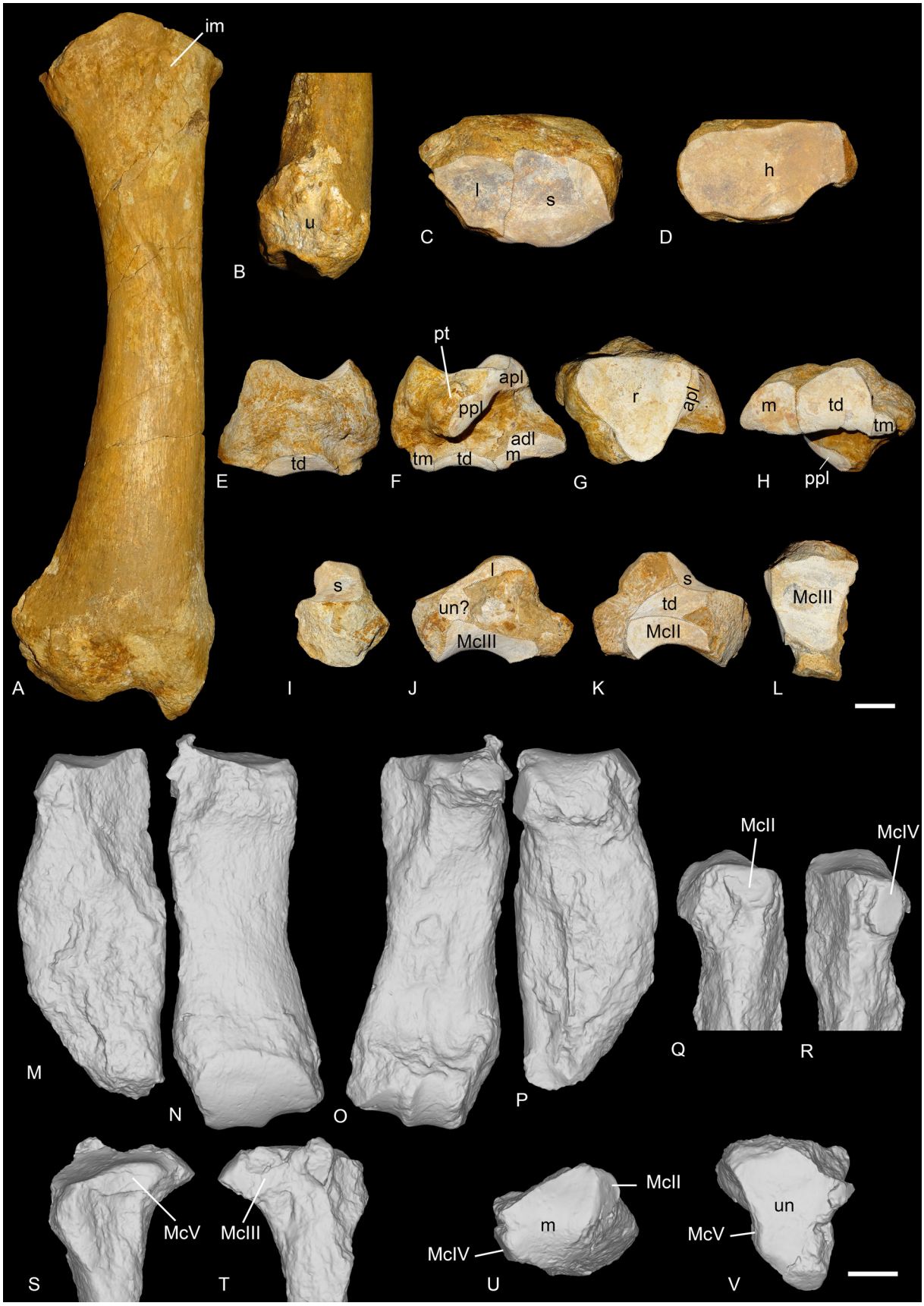
im
A
u
B
l
s
C
h
D
td
E
pt
apl
ppl
adl
tm
td
m
F
r
apl
G
m
td
tm
ppl
H
s
I
l
un?
McIII
J
s
td
McII
K
McIII
L
McII
McIV
Q
R
M
N
O
P
McV
McIII
S
T
McII
m
McIV
U
un
McV
V

the pisiform and a laterally reduced facet for the ulna. On the medial side, the two facets for the lunate are very small, band-shaped and anteroposteriorly elongated, contrary to the pyramidal of *Ronzotherium*.

Trapezoid. Two trapezoids are preserved from 'Marseille' (FSL-9501 and FSL-520283, Fig. 18B). In anterior view, they are wider than high. The proximal border is sigmoid on the specimens from 'Marseille'. The magnum facet occupies the whole lateral side, while the medial side is partly occupied by the extension of the scaphoid facet, and by a subtriangular medio-distal articulation for the trapezium. The proximal side is fully occupied by the anteroposteriorly concave scaphoid facet. The distal articulation for the McII is anteroposteriorly concave.

Fig. 20. *Ronzotherium romani* Kretzoi, 1940 from Gaimersheim (late Oligocene, Germany). – **A–F**. Left astragalus (BSPG collection). **A**. Anterior view. **B**. Posterior view. **C**. Lateral view. **D**. Medial view. **E**. Distal view. **F**. Proximal view. – **G–K**. Left MtIII BSPG-1952-II. **G**. Anterior view. **H**. Posterior view. **I**. Lateral view. **J**. Medial view. **K**. Proximal view. Abbreviations: c = cuboid; Cc1 = calcaneus facet 1; Cc2 = calcaneus facet 2; Cc3 = calcaneus facet 3; ct = collum tali; ec = ectocuneiform; f = fibula; ll = lateral lip; ml = medial lip; n = navicular; t = tuberosity. Scale bar: 2 cm.

Comparison. The only other known trapezoid of *Ronzotherium* belongs to *R. filholi* from Villebramar (Brunet 1979). It differs by a flattened distal articulation for the McII and a concave proximal border in anterior view. This trapezoid is also smaller than those that we refer here to *R. romani*, especially anteroposteriorly. Because we lack comparative specimens, especially with the type species *R. velaunum*, we can only tentatively attribute these trapezoids to *R. romani*.

Magnum. It is preserved from Gaimersheim (BSPG collection, Fig. 19I–L) and Rickenbach (NMO-H10/110, Fig. 21J). The specimens are partly broken. In anterior view, the proximal border is straight. The anterior side is wider than high. The proximal apophysis is wide, high and very convex. This apophysis is laterally bordered by a long band-shaped articulation for the lunate, that completely fuses anteriorly with the small unciform facet. The proximomedial facet for the scaphoid is larger and concave anteroposteriorly. This facet is very poorly distinguished from the medial facet for the trapezoid. This latter facet is longer than high, and its morphology would fit the shape of the corresponding facet on the trapezoid from 'Marseille'. The trapezoid facet is separated from the medio-distal McII facet by a ridge and by a very short and shallow notch anteriorly. This facet is much longer than high, flat and its distal border is very concave in medial view. On the distal side, the McIII facet is large, trapezoidal, longer than wide and very concave anteroposteriorly. The posterior tuberosity of the magnum is short and straight in Rickenbach.

Comparison. The magnum of *R. velaunum* PUY.2004.6.263.RON differs from the specimens from Rickenbach and Gaimersheim by its narrower proximal apophysis. The magnum of *R. filholi* also differs from *R. romani* by its higher and narrower anterior side. The magnum of *Diaceratherium asphaltense* (FSL-213008) only differs by a slightly longer and straighter posterior tuberosity, and by a shorter proximal contact between the trapezoid and scaphoid facets.

Unciform. Three unciforms (FSL-520289, FSL-520282 and NMB-Mar-865, Fig. 18C) are preserved from 'Marseille' according to Ménouret & Guérin (2009) but we only could recover the specimen NMB-Mar-865. It is almost complete, only a small part of the anterolateral side is missing. In anterior view, the two proximal facets for the pyramidal and the lunate are visible. In proximal view, the posterior expansion of the pyramidal facet was probably absent, and the pyramidal and McV facets were probably separated. The McV facet is large, very concave and located posteriorly. The posterior apophysis is thin, curved and 'hook-shaped'. In distal view, the McIII and McIV facets are almost undistinguishable, forming a single large convex facet.

Comparison. Only one other unciform of *Ronzotherium* is known, from Ronzon, but it is very incomplete. However, from the remaining part, the dimensions are very similar to those of *R. romani*, and no characters permit to distinguish them. In contrast, the unciform of *Diaceratherium tomerdingense* (SMNS-16157e) strongly differs from that of *R. romani* by its very wide and flattened posterior apophysis, its larger McV facet contacting the pyramidal facet, the much thinner and elongated McIII facet that is well distinguished from the McIV facet and the anteroposteriorly concave McIV facet. The unciform of *D. lemanense* (MNHN-LIM-598) also has a very wide posterior apophysis and a connection between the McV and pyramidal facets. The unciform of *D. aginense* (MHNM.1996.17.98) shows a similar wide posterior apophysis, but the contact between the pyramidal and the McV facets is absent.

McIII. The McIII is overall very badly preserved. In 'Marseille', UPM-13667 is incomplete and poorly preserved, whereas FSL-9505 and FSL-520281 are two proximal extremities (none found in collection). In Gaimersheim (BSPG collection, Fig. 19M, P–R, U), it is very broken and incomplete. The anterior McII facet is large and semi-circular. The posterior McII facet seems absent. The magnum facet is convex anteroposteriorly. On the lateral side, only the posterior McIV facet is preserved, but it was separated from the anterior by a shallow groove.

Comparison. The McIII of *R. velaunum* is unknown. One McIII of *R. filholi* is preserved in Möhren 7 (BSPG-1969-XXIV) and differs by the much smaller anterior McII facet. However, the posterior McIV facet is similar and also separated by a shallow groove from the anterior. This groove is larger in Villebramar (Brunet 1979). The McIII of *Diaceratherium* cannot be distinguished based on these characters.

McIV. It is preserved from 'Marseille' (FSL-520287, NMB-Mar-863 and NMB-Mar-864, Fig. 18D), Gaimersheim (BSPG collection, Fig. 19N–O, S–T, V) and Rickenbach (NMO-I8/117, Fig. 21K). In proximal view, the proximal side is lozenge to triangular-shaped. The articulation for the unciform is almost flat anteroposteriorly, but slightly concave lateromedially. On the lateral side, the articulation for the McV is long and low, except on the specimen from Rickenbach where it is reduced and circular. The rugosity of the contact surface for the McV on the lateral border occupies almost half of the diaphysis proximally. On the medial side, two large facets articulate with the McIII (broken on the specimen from Gaimersheim): one is band-shaped and anteroposteriorly elongated on the anteroproximal border, and the other oval-shaped, posterior and separated from it by a groove. These two facets are almost in the same vertical plane. In posterior view, the specimen from Rickenbach differs from the others by its very deep fossa, just above the distal articulation.

Comparison. The McIV of *Diaceratherium tomerdingense* (SMNS-16155b) strongly differs by its reduced length (only 9.5 cm), its convex medial border of the diaphysis with a prominent rugose tuberosity on the anteroproximal part of the diaphysis, the anterior McIII facet contacting the posterior one and the deep incision of the posterior border of the unciform facet in proximal view. The McIV of *D. asphaltense* (FSL-213012) also differs by its convex medial border of the diaphysis with a prominent rugose tuberosity on the anteroproximal part of the diaphysis, but the two McIII facets are separated, and the unciform facet is not incised.

Sacrum. A sacrum is preserved from Poillat (MJSN-BEU-001-280). It is quite well preserved and is formed by the fusion of five sacral vertebrae. The neural spines are not fused together and there are four dorsal and ventral sacral foramina on each side.

Comparison. Because of the rarity of the preservation of the sacrum, no comparison can be made, either with other ronzotheres or with *Diaceratherium*.

Fig. 21 (next page). *Ronzotherium romani* Kretzoi, 1940 from Rickenbach (late Oligocene, Switzerland). – **A**. Mandible NMB-UM-3832. **A1**. Occlusal view. **A2**. Lateral view. **A3**. Lingual view. – **B**. Left P2 NMB-Ri-24. **B1**. Occlusal view. **B2**. Lingual view. – **C**. Left P4 NMO-H9-13. **C1**. Occlusal view. **C2**. Lingual view. – **D**. Right P4–M1 NMB-UM-1840. **D1**. Occlusal view. **D2**. Lingual view. – **E**. Left M2 NMB-Ri-27. **E1**. Occlusal view. – **F**. Left M2–3 (SMNS collection). **F1**. Occlusal view. – **G**. Left scaphoid NMO-I5-62. **G1**. Medial view. **G2**. Proximal view. **G3.** Lateral view. **G4**. Distal view. – **H**. Right lunate NMO-I7-115. **H1**. Anterior view. **H2**. Proximal view. **H3**. Distal view. **H4**. Lateral view. **H5**. Medial view. – **I**. Right pyramidal NMO-I11-82. **I1**. Anterior view. **I2**. Medial view. **I3**. Proximal view. **I4**. Distal view. – **J**. Left magnum NMO-H10-110. **J1**. Anterior view. **J2**. Medial view. **J3**. Distal view. **J4**. Lateral view. – **K**. Right McIV NMO-I8-117. **K1**. Anterior view. **K2**. Medial view. **K3**. Lateral view. **K4**. Proximal view. – **L**. Left MtII NMB-UM-2565. **L1**. Proximal view. **L2**. Anterior view. **L3**. Lateral view. Abbreviations: adl = anterodistal facet for the lunate; apl = anteroproximal facet for the lunate; ec = ectocuneiform; l = lunate; m = magnum; mc = mesocuneiform; p = pyramidal; pi = pisiform; ppl = postero-proximal facet for the lunate; r = radius; s = scaphoid; td = trapezoid; tm = trapezium; ul = ulna; un = unciform. Scale bar: 2 cm.

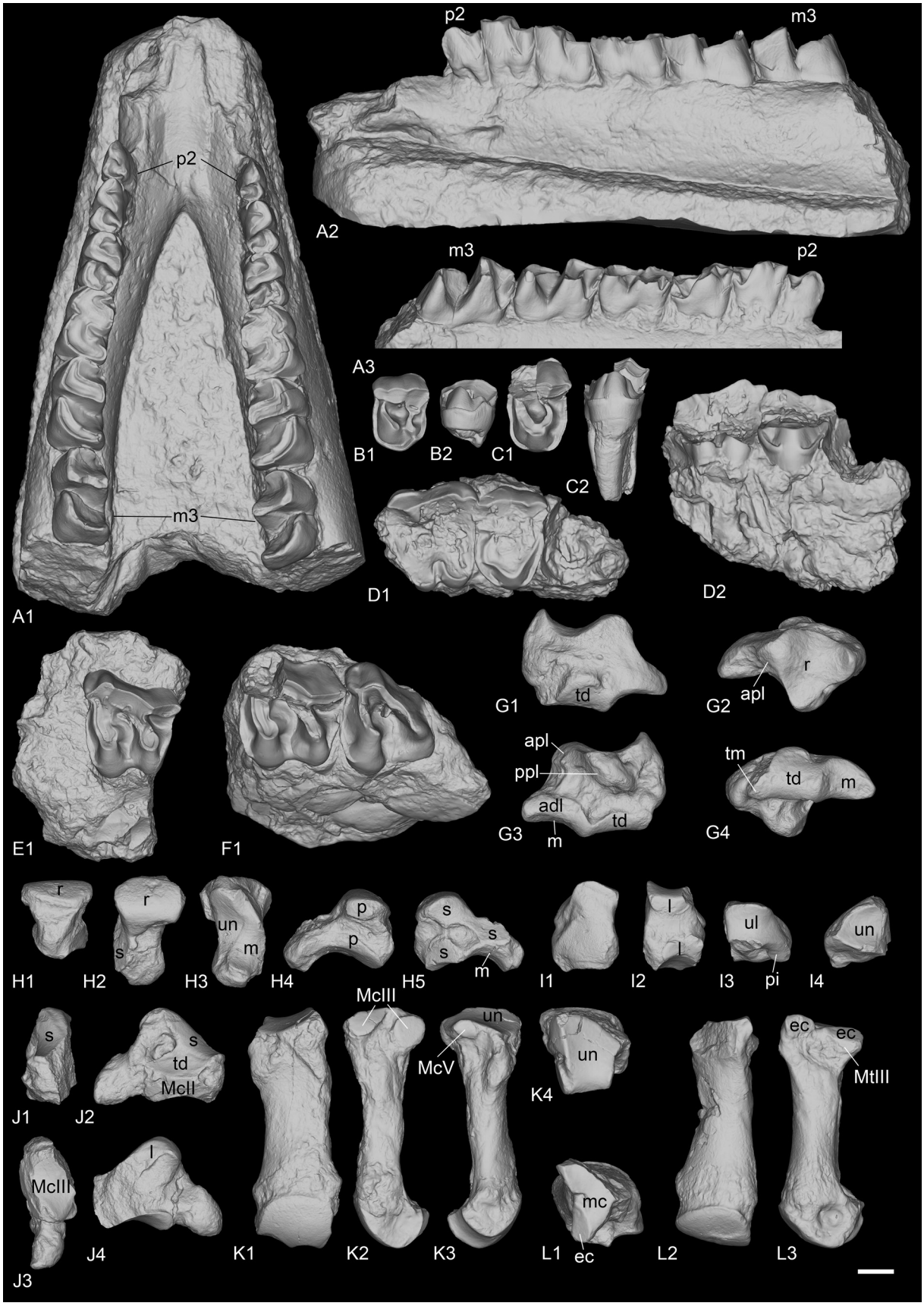
p2
m3
A2
m3
p2
A3
p2
m3
A1
B1
B2
C1
C2
D1
D2
E1
F1
G1
td
G2
r
apl
apl
ppl
adl
td
m
G3
tm
td
m
G4
r
r
s
un
m
p
p
s
s
s
m
l
l
ul
pi
un
H1
H2
H3
H4
H5
I1
I2
I3
I4
s
s
td
McII
McIII
un
McV
un
K4
ec
ec
MtIII
J1
J2
l
McIII
mc
J4
J3
K1
K2
K3
L1
ec
L2
L3

Femur. Only a very poorly preserved but subcomplete femur is known from the locality of Poillat (MJSN-POI007-80). The distal articulation is only known in 'Marseille' (NMB-Mar-828, Fig. 18E). The head of the femur is rounded, and the fovea capitis is deep. The smaller trochanter is only preserved on the specimen from Poillat, and it is very small. The third trochanter, the medial condyle and the medial lip of the trochlea are not preserved. The lateral condyle is protruding posteriorly, far behind the diaphysis and the lateral epicondyle is present but not very developed laterally.

Comparison. There are almost no characters preserved that permit to distinguish the femur of *R. romani* from other ronzotheres, or from *Diaceratherium* but it is overall very similar to the femur of *R. velaunum* from Ronzon.

Tibia. It is only known from Gaimersheim (BSPG collection), and only its medial half is preserved. The medial articulation surface is circular and concave in proximal view and the medial intercondylar tubercle is present. The medial border of the diaphysis is slightly concave. In the distal part, the mediodistal gutter is not preserved and the posterior apophysis is broken. The ridge delimitating the two distal condyles is wide and low. The fibula is unknown.

Comparison. Based on what is left from this tibia, it only seems to differ from *Ronzotherium velaunum* (PUY.2004.6.260.RON and PUY.2004.6.261.RON) in having a larger size. However, it is slightly shorter than the tibiae of *R. filholi* from Villebramar. There are too few characters visible on the tibia from Gaimersheim to compare it with those of *Diaceratherium*, which also have a very similar size.

Astragalus. It is preserved from Gaimersheim only (BSPG collection, Fig. 20A–F) and slightly eroded but complete. It is wider than high (TD > H) and its APD/H ratio is high (around 0.78). On the lateral side, the fibula facet is large, flat and vertical. In anterior view, the lateral lip is larger than the medial one, and the groove between the two lips is wide. The collum tali is very high, the two lips of the trochlea do not contact the distal articulation at all. The distal articulation for the navicular is concave in anterior view. In distal view, this articulation is a parallelogram, and it bears a proximal extension on the posterior side of the astragalus. Lateral to the articulation for the navicular, there is a smaller, almost flat and anteroposteriorly elongated facet for the cuboid. This facet is posteriorly broken, and the posterior stop is thus not preserved. In distal view, the trochlea is oblique compared to the distal articulation. In proximal view, the posterior border of the trochlea is sinuous. In posterior view, the three facets for the calcaneum, Cc1, Cc2 and Cc3, are distinct. The Cc1 facet is the largest and it bears a low and wide distal extension on the lateral side. It is rather triangular, and almost flat in lateral view. It is separated from the Cc2 by a deep proximal fossa, and from the Cc3 facet by a wide groove. The Cc2 facet is almost contacting the Cc3 facet by a very thin bridge and it is oval-shaped and slightly proximodistally elongated. There is a strong, rounded tuberosity medial to this Cc2 facet and separated by a large and deep proximodistal groove. Distally, the Cc3 facet is low and band-shaped, but partly eroded. The medio-distal tubercle of the astragalus is broken.

Comparison. The astragalus of *R. velaunum* (PUY.2004.6.1770.RON) shares with the astragalus of *R. romani* the very high collum tali and the absence of contact between the trochlea and the distal border, the large lateral lip compared to the medial one, the wide groove between the two lips of the trochlea, the large and flat fibula facet, the transversally concave distal navicular facet and the oblique trochlea compared with the distal articulation, in distal view. These same characters are also found on the astragalus of *R. filholi* from Villebramar. Unfortunately, the posterior side of the astragalus of *R. velaunum* is still in sediment. Another astragalus (MNHN.LIM7) attributed to *R. filholi* from Bournoncle-Saint-Pierre is also very similar but it shows an even more laterally offset lateral lip of the trochlea. It shares, however, the deep proximal fossa separating the Cc1 and Cc2 facets, the oval-shaped and proximodistally elongated Cc2 facet, and the band-shaped Cc3 facet. However, on this specimen, the Cc1 facet is very concave in

lateral view and the Cc2 facet is connected to the Cc3 by a very wide band, contrary to the specimens from Gaimersheim and Villebramar (flattened sagittally). Also, the distal extension of the Cc1 facet is long, thin and drop-shaped. The astragalus of *Diaceratherium lemanense* from Gannat (NMB-Gn-158), as well as the astragali of *D. aginense* from Laugnac (MHNM.1996.17.41, -.55 and -.77) differ from the astragalus of *R. romani* in having a more visible and more concave facet for the navicular in anterior view, a lower height, a lower collum tali, more rounded lips of the trochlea, a larger and circular Cc2 facet, completely independent Cc2 and Cc3 facets, a concave Cc1 facet in lateral view and a reduced distal extension of the Cc1 facet.

The calcaneum, meso- and entocuneiform remain unknown for *R. romani*.

Navicular. It is only preserved in 'Marseille' (NMB-Mar-847e, Fig. 18F). It is quite large, longer than wide and pretty high. The proximal articulation for the astragal is slightly anteroposteriorly concave and occupies the whole anterior side. The distal side is occupied by two poorly distinguished facets: a large, anterolateral and almost triangular one for the ectocuneiform, and a smaller one, rectangular and located postero-medially, for the mesocuneiform. There is possibly a third very small facet for the entocuneiform, but it cannot be distinguished from the mesocuneiform facet. On the lateral side, there is a single posterior and convex articulation for the cuboid. The cross-section of the navicular is lozenge-shaped.

Comparison. The navicular of *Ronzotherium velaunum* is not preserved from Ronzon, but one specimen is known in Haag 2 (unnumbered in BSPG collection). It shares a very similar shape in proximal view, with a distinct posterior notch, as well as the absence of an anterior cuboid facet and a similar concavity in lateral view. The only other known navicular of *Ronzotherium* belongs to *R. filholi* from Villebramar (Brunet 1979). Its morphology is very similar and it basically only differs by its slightly smaller size. The navicular of *D. lamilloquense* (Michel 1983) differs by its shape, it is as long as wide, and by the presence of an anterolateral facet for the cuboid. It also differs by its distal facets: the mesocuneiform facet is triangular and slightly convex, the entocuneiform facet is oblique, and the three cuneiform facets are distinguishable and separated. The navicular of *D. aginense* is also as wide as long and differs by its distal articulation surfaces. The navicular of *D. aurelianense* (Cerdeño 1993) also differs by its overall shape, by the two facets for the cuboid, and by a strong angle between the distal ento- and mesocuneiform facets.

Ectocuneiform. Only one ectocuneiform is known for *R. romani*, from 'Marseille' (NMB-Mar-735, Fig. 18H). The proximal articulation for the navicular is roughly triangular, concave and longer than wide. The postero-lateral process is absent. The lateral side bears two facets for the cuboid, a large and oblique anterodistal one, and a smaller postero-proximal one. The groove separating these two is rather deep. On the medial side, the mesocuneiform facet is thin, low, elongated and located postero-proximally whereas the two distal articulations for the MtII are rather large. The anterior one is concave whereas the posterior one is larger and convex. The distal articulation for the MtIII is triangular. In anterior view, the distal border is sinusoidal.

Comparison. The ectocuneiform of *R. velaunum* (PUY.2004.6.577.RON) slightly differs by its smaller and vertical anterodistal facet for the cuboid and its smaller posterior facet for the MtII. The ectocuneiform of *R. filholi* from Villebramar (Brunet 1979) only differs by its slightly smaller size. The ectocuneiform of *Diaceratherium* greatly differs from *Ronzotherium*. The ectocuneiform of *D. lamilloquense* from La Milloque (Michel 1983) differs by the presence of a facet for the MtIV below the anterior facet for the cuboid and by a less elongated and triangular facet for the mesocuneiform, that is located more anteriorly than in *Ronzotherium*. The ectocuneiform of *D. lamilloquense* from Castelmaurou (Duranthon 1990)

differs by the presence of a third articulation facet for the cuboid. The one of *D. aurelianense* from Artenay differs by the fusion of the two distal facets for the MtII (Cerdeño 1993).

Cuboid. It is preserved in 'Marseille' (FSL-9528 and NMB-Mar-847d, Fig. 18G). The anterior side is approximately as high as wide. In anterior view, the proximal articulation is posteriorly elevated. In proximal view, the posterior apophysis is almost not visible, the proximal side is occupied almost exclusively by the two articulation surfaces, for the astragalus on the medial side, and for the calcaneus laterally. The proximal side is trapezoid and the astragalus and calcaneal facets are almost equal-sized. On the medial side, the postero-proximal and elongated facet for the navicular is concave and contacts the small, square and postero-mesial facet for the ectocuneiform. The navicular facet bears a thin extension up to the anterior border, bordering the astragalus facet. The small anterodistal facet for the ectocuneiform is separated from the posterior one by a wide groove. On one specimen (NMB-Mar-847d), this anterodistal facet is very developed and deeply concave, with a strong medial extension, that is not visible on the other specimen. There is no articulation facet on the lateral side, but a large and deep groove, obliquely and forward oriented, which serves as a 'slideway' for the tendon of the m. fibularis longus and isolates the posterior apophysis of the cuboid from the main body of the bone. In distal view, the distal articulation for the MtIV is almost flat and triangular.

Comparison. The cuboid of *R. velaunum* (PUY.2004.6.1309.RON and PUY.2004.6.268.RON) differs from that of *R. romani* by its smaller and oval-shaped distal articulation for the MtIV, by its shallow groove separating the proximal calcaneal facet from the astragalus one, and by its slightly shorter proximal articulation. All other characters are overall very similar to those of *R. romani*. The cuboid of *R. filholi* from Villebramar is poorly preserved, but it differs nonetheless by its slightly shorter posterior height, at the level of the posterior apophysis. The cuboid from the Quercy (NMB-QE-362) tentatively referred to ?*R. filholi* differs by its very different morphology of the anterior side, the absence of ridge separating the proximal astragalus and calcaneal facets and its more posteriorly elevated proximal articulation, but resembles *R. romani* by its very similar medial articulations for the ectocuneiform and navicular. The cuboid of *Diaceratherium asphaltense* (FSL-213014) from Pyrimont-Challonges greatly differs from *R. romani* by its proportions, dimensions and morphology (see Depéret & Douxami 1902: pl. XXIX, fig. 7). It differs by the presence of an isolated anteroproximal facet for the lunate. The height of the anterior side is much smaller than in *R. romani*, whereas its width is similar. However, it is much higher posteriorly than the cuboids of *R. romani*, because of the very high apophysis, and the strong posterior elevation of the proximal surface. The proximal articulation is rectangular in proximal view and the posterior apophysis is very visible posterior to this articulation. The distal articulation for the MtIV is transversally convex and concave anteroposteriorly. The lateral groove for the tendons is very shallow. Another cuboid from Castelmaurou (TLM.PAL.2014.0.2563) attributed to *D. lamilloquense* (Duranthon 1990) also shares the same characters as *D. asphaltense*, and especially the isolated anteroproximal facet for the lunate, which is always absent in ronzotheres. The presence of this facet thus seems to be a diagnostic character differentiating *Diaceratherium* from *Ronzotherium*.

MtII. One MtII of *R. romani* is preserved from 'Marseille' (NMB-Mar-847a, Fig. 18I) but was originally attributed to a McII of "*Diaceratherium*" *massiliae* and another from Rickenbach (NMB-UM-2565, Fig. 21L). It is partly broken proximally. In anterior view, the proximal articulation for the mesocuneiform is concave. The diaphysis is curved towards the medial side and is very widened distally. Antero-laterally, there is no anterior articulation for the MtIII, only a single small facet for the ectocuneiform. A groove separates this facet from the two posterior facets (not preserved on the specimen from 'Marseille'): one is for the ectocuneiform, the other below, is for the MtIII. The ectocuneiform facet is large and oblique, whereas the MtIII facet is thin and elongated.

Comparison. The MtII of *R. filholi* from Villebramar (Brunet 1979) and Möhren 7 (BSPG-1969-XXIV-73) differ by the presence of an anterior facet for the MtIII, below the ectocuneiform facet, and by their gracility. The MtII of *D. lemanense* from Wischberg (Jame *et al.* 2019) differs in being more gracile, but also in having a very large posterior facet for the ectocuneiform, an anterior facet for the MtIII and an elongated posteromedial entocuneiform facet.

MtIII. It is only preserved from Gaimersheim (BSPG-1952-II, Fig. 20G–K). It differs drastically from MtIII of *R. filholi* from Villebramar by its robustness. The proximal part is slightly broken medially and laterally. The proximal articulation for the ectocuneiform is roughly trapezoid, with a lateral notch separating the two facets for the MtIV, and it is as wide as long. It is slightly bulged at the level of this notch. There is no facet for the cuboid. In anterior view, the proximal border is straight and oblique and there is a marked distal widening of the diaphysis towards the distal articulation. In medial view, the anterior articulation for the MtII is broken but may have been absent, and the posterior is small and poorly differentiated from the proximal articulation. In lateral view, the anterior articulation for the MtIV is large and triangular, whereas the posterior is poorly preserved. They are separated by a deep groove. The distal keel is quite smooth but still visible in anterior view, and there is no distal tubercle on the posterior side. The insertions of the m. interossei are long on the medial and lateral sides (they extend beyond the middle of the diaphysis).

Comparison. The MtIII of *R. velaunum* is poorly preserved, and it differs from that of *R. romani* by its greater length, even though its width is quite similar. It also shares with *R. romani* a distal widening of the diaphysis and a smooth distal keel of the articulation. The MtIII of *R. filholi* from Villebramar differs from that of *R. romani* by its higher gracility, but it shows a similar distal widening of the diaphysis. As in *R. romani*, the proximal border is straight and oblique in anterior view and the distal keel is smooth. Another MtIII from Möhren 7 (BSPG-1969-XXIV-156) is quite similar to that of *R. romani*, as it shares the distal widening of the diaphysis, the absence of a posterior facet for the MtII, the presence of a posterior articulation for the MtII and the similar shape of the proximal side. Although their length is almost equal, the MtIII of *R. romani* is much wider. The MtIII of *Diaceratherium asphaltense* (FSL-213016) differs by its smaller size and its reduced width, compared to the MtIII of *R. romani*. The shape of the proximal side in anterior view is also quite different, it is triangular. It also differs by its shorter insertion for the m. interossei, the absence of a posterior facet for the MtII and the absence of distal widening of the diaphysis. In proximal view, the anterior border of the proximal articulation is straight, and it is also slightly less oblique in anterior view. The MtIII of *D. lamilloquense* from Castelmaurou (TLM.PAL.2014.0.2564) differs from that of *R. romani* by its much thinner diaphysis, its concave proximal articulation in anterior view, the absence of a posterior facet for the MtII, and its proximal side being much wider than long in proximal view.

MtIV. It is only preserved from ‘Marseille’ (FSL-520286, Fig. 18J), and it is complete. As for the MtIII, it is also more robust than the MtIV of *R. filholi* from Villebramar. The proximal articulation for the cuboid is roughly triangular, with a small notch on the medial side between the two facets for the MtIII. The postero-proximal tuberosity is pad-shaped and continuous. On the medial side, the two facets for the MtIII are rather large, and separated by a narrow groove, than runs from the proximal side to the anterior side. The anterior MtIII facet is triangular while the posterior one is less proximal, and oval-shaped. There is no posterior tubercle. The MtV facet is absent. By virtually articulating the 3D models of this MtIV to the MtIII from Gaimersheim, their morphologies would both match very well: the length of the anterior MtIII/MtIV facet is identical, and the groove is located at the same position; on the diaphysis, the insertions for the m. interossei extend up to the same level.

Comparison. The MtIV of *R. velaunum* from Ronzon is lost. The MtIV of *R. filholi* from Villebramar (Brunet 1979) differs by its dimensions, the concave proximal facet for the cuboid, and the much wider

groove separating the two MtIII facets. The MtIV of *Diaceratherium lamilloquense* (Duranthon 1990) also differs by its dimensions, by the concave proximal facet for the cuboid, by the much wider groove separating the two MtIII facets and by the 90° angle between these two. The MtIV of *D. aginense* from Laugnac (de Bonis 1973: fig. 34a) further differs by the presence of an anterior ectocuneiform facet, by a reduced postero-proximal tuberosity and by the very different shape (triangular) of the proximal side.

Final remarks. All these newly identified postcranial remains considerably change our view of the species *Ronzotherium romani*. Prior to this study, only scarce remains were identified, and this species was believed to resemble its closely-related species *R. filholi*, by being rather medium-sized, gracile and cursorial. Based on this wrong premise, large and robust postcranial rhinocerotid remains from 'Marseille' were not assigned to the co-occurring *R. romani*. Indeed, the species, "*Diaceratherium*" *massiliae* was named based on these short and robust postcranials, as it was not conceivable to consider they would document any representatives of *Ronzotherium* (Ménouret & Guérin 2009). Yet, by comparing postcranial remains to other remains of *Ronzotherium*, especially to those of *R. velaunum* for which the postcranial skeleton is well preserved, we show that all of them can be assigned to *Ronzotherium*, instead of *Diaceratherium*. In particular, the postcranial skeleton of *Ronzotherium romani* differs from *Diaceratherium* by:

- the lower fossa olecrani of the humerus in posterior view and the constricted condyles in anterior view;
- the equal posterior and anterior heights of the scaphoid, a less convex dorsal border in proximal view, a concave distal articulation for the magnum, a less concave articulation for the trapezoid and a smaller articulation for the trapezium;
- the large posterior tuberosity of the lunate in proximal view, the developed posterior extension of the proximal facet for the radius, the higher anterior side in anterior view, the shallower groove separating the anteroproximal facet for the scaphoid from the postero-proximal, as well as the reduced anterior portion of the facet for the magnum (it is almost as large as the distal pyramidal facet);
- the higher anterior side of the pyramidal, the more elongated facet for the pisiform, the developed facet for the ulna and the larger facets for the lunate;
- the shorter and straight posterior tuberosity of the magnum and a shorter proximal contact between the trapezoid and scaphoid facets;
- the thin, curved and 'hook-shaped' posterior apophysis of the unciform, the larger McIII facet, poorly distinguished from the McIV facet and the convex McIV facet;
- the absence of rugose tuberosity on the anteroproximal part of the diaphysis of the McIV, the straighter medial border of the diaphysis and its more reduced robustness;
- the less concave facet for the navicular on the atragalus, the higer collum tali, the smaller Cc2 facet, the contact between the Cc2 and Cc3 facets, a flatter Cc1 facet in lateral view and the large distal extension of the Cc1 facet;
- the global size and shape of the navicular, longer than wide, and its single posterior articulation for the cuboid;
- the disposition of the facets of the ectocuneiform;
- the absence of anteroproximal facet for the lunate on the cuboid and the trapezoid proximal side;
- the more robust MtII, without anterior facet for the MtIII;
- the wider diaphysis of the MtIII and the different shape of its proximal articulation;
- the dimensions of the MtIV and the shallower groove separating the two MtIII facets.

Accordingly, *Diaceratherium massiliae* Ménouret & Guérin, 2009 should be considered as a junior synonym of *Ronzotherium romani* Kretzoi, 1940.

Ronzotherium heissigi sp. nov.
urn:lsid:zoobank.org:act:D1CFA5AE-6BC9-479B-AE43-F46EB9D86A49
Figs 22–26

Acerotherium lemanense – Roman 1912a: 61–62, pl. VII (from Lamothe-Capdeville).
Aceratherium filholi – Stehlin 1914: 183, 85 (Bumbach).
Ronzotherium filholi – Lavocat 1951: 116, pl. 19 fig. 3, pl. 26 fig. 1 (from Vendèze). — Brunet 1979: 105 (from Bumbach). — Becker 2003: 213–214.
Ronzotherium velaunum – Heissig 1969: 20–36, 77, fig. 8b (from Vendèze).
Ronzotherium filholi elongatum – Heissig 1969: 46–55, 71, 75–77, 82–83 (from Bumbach).
Ronzotherium filholi romani – Heissig 1969: 63 (from Lamothe-Capdeville).
Ronzotherium romani – Brunet 1979: 135–136, fig. 15, pls XVII–XVIII (from Vendèze).
Diaceratherium lemanense – Antoine & Becker 2013: 140 (from Lamothe-Capdeville).

Diagnosis

Differs from *R. romani* by the mandibular ramus inclined forward, the P1 sometimes absent and without anterolingual cingulum, the angular and V-shaped external groove of the lower cheek teeth, the lower premolars without lingual cingulum, the d/p1 always absent in the adult, the deep and wide gutter for the m. extensor carpi on the radius, the concave proximal border of the anterior side of the magnum, the salient insertion of the m. extensor carpalis of the metacarpals and the oval proximal side of the cuboid.

Differs from *R. velaunum* by the presence of a lingual groove on the corpus mandibulae, the curved and not constricted paralophid on p2 and the deep median constriction of the distal humeral articulation.

Differs from *R. filholi* by a foramen infraorbitalis above P3, a zygomatic width/frontal width ratio above 1.5, a concave occipital crest, the reduced paraconid on p2, the high posterior expansion of the scaphoid facet on the radius, the open angle between the diaphysis of the ulna and the olecranon and the curved magnum facet on the McII.

Differs from *R. elongatum* by the absence of processus lacrymalis, the reduction of the postorbital process on the zygomatic arch, its poorly developed processus posttympanicus and by the metaloph of P2 directed postero-lingually.

Further differs from *R. filholi* and *R. elongatum* by a convex processus postglenoidalis of the squamosal and by a narrow and V-shaped lingual opening of the lower premolars.

Etymology

The specific epithet honours Prof. Dr Kurt Heissig for his major and imperishable contributions on the study of the Rhinocerotidae, and for providing the first systematic revision on *Ronzotherium* more than 40 years ago.

Type material

Holotype

FRANCE • complete skull and associated mandible; Auvergne-Rhône-Alpes, Cantal, Vendèze near St-Flour; 45°02′36.8″ N, 3°06′13.1″ E; MNHN.F.LIM181.

According to the MNHN registry, it was discovered by M. Lauby (possibly Antoine Lauby), but sold to the MNHN by M. Hugon, from St-Flour on the 19th of June 1909. It bears the old MNHN inventory number MNHN.F.1909-25.

Additional material

SWITZERLAND – **Bumbach (MP25)** • 1 very poorly preserved and incomplete skull; NMB-UM-200 • 1 fragment of parietal bone with occipital crest; NMBE-5035820 • 1 P1; NMB-UM-463 • 1 P2; NMB-UM-126a • 1 P2; NMBE-5014494 • 1 P3; NMBE-5035822 • 1 P3; MGL-4264 • 2 P4; MGL-5265, MGL-5266 • 1 M2; NMBE-5014495 • 1 subcomplete mandible; NMB-UM-6132 • 1 d2; MGL-5275 • 1 d4; NMB-UM-13 • 1 p2; NMBE-5035824 • 1 p3; MGL-5274 • 1 fragment of mandible with p3–4; NMBE-5035825 • 2 p4; NMBE-5035826, NMBE-5035827 • 1 p4; NMB-UM-6133 • 1 m1; NMB-UM-806 • 1 m1; NMBE-5035828 • 1 m2; NMB-6278 • 3 m2; NMBE-5035829, NMBE-5035830, NMBE-5035831 • 1 m3; NMBE-5035832 • 2 incomplete humeri; NMB-UM-132, NMB-UM-129a • 1 radius; NMB-UM127a • 1 ulna; NMB-UM-131b, NMB-UM-131c • 1 lunate; NMBE-5035833 • 2 trapezoids; NMB-UM-6136b, NMB-UM-6 • 1 magnum; NMB-UM-6136c • 1 McII; NMB-UM-6136a • 1 McII; NMB-UM-121 • 1 proximal fragment of femur; NMBE-5035835 • 1 cuboid; NMBE-5035834.

Type horizon and locality

Vendèze near St-Flour, Cantal, Auvergne-Rhône-Alpes, France (MP24, late early Oligocene), approximative coordinates: 45°02′36.8″ N, 3°06′13.1″ E.

Stratigraphical distribution

MP24–MP25.

Geographical distribution

France: 'Auvergne' (without precision, which could possibly correspond to Vendèze), Lamothe-Capdeville, Vendèze. Switzerland: Bumbach.

Description

Holotype

Skull. The skull MNHN.F.LIM181 is quite well preserved but the nasals are broken (Figs 22–23). The premaxillae are long and contact each other only at their anterior extremity. The nasal notch extends up to P2 and the foramen infraorbitalis is located above P3. The nasal septum is not ossified. The suture between the nasals and the lacrimal is not visible and the lacrimal process is absent. The orbit is large and its anterior border is above the anterior side of M1. The processus postrobitalis of the frontal is large. The anterior base of the zygomatic process is high above the teeth neck. The zygomatic arch is high in lateral view, it is almost reaching the dorsal border of the skull. The postorbital process of the zygomatic arch is almost absent and very poorly distinguishable. The dorsal profile of the skull is overall concave in lateral view. The external auditory pseudomeatus is partially closed and the occipital side is inclined forward. The nuchal tubercle is developed. The back of the teeth row is in the posterior half of the skull in lateral view. In dorsal view, the skull is brachycephalic and it is hornless. The orbit is not laterally projected. The zygomatic width/frontal width ratio is above 1.5. A very thin sagittal crest is present, and the occipital crest is not preserved. In ventral view, the anterior tip of the zygomatic arch diverges progressively from the maxilla, without a sharp angle. The vomer and most of the basicranium are not preserved. The articular tubercle of the squamosal is rather smooth and its transverse profile is straight. The anterolateral sides of the processus postglenoidalis form a right dihedron. There is no posterior groove on the zygomatic process. The processus posttympanicus and paraoccipitalis are fused at their base. The processus post-tympanicus is poorly developed while the paraoccipitalis is developed. The foramen magnum is circular and there are no median ridges on the condyles, neither medial truncation.

Mandible. The mandibular symphysis (Fig. 24A–B) is slightly upraised and it is long and massive in dorsal view. Its posterior margin is at the level of p2. There are two mental foramen, one bellow p2 and one below the root of i2. The lingual groove of the sulcus mylohyoideus is slightly marked on the lingual

Fig. 22. *Ronzotherium heissigi* sp. nov. from Vendèze (late early Oligocene, France). Skull MNHN.F.LIM181. **A**. Dorsal view. **B**. Left lateral view. **C**. Ventral view. Scale bar: 2 cm.

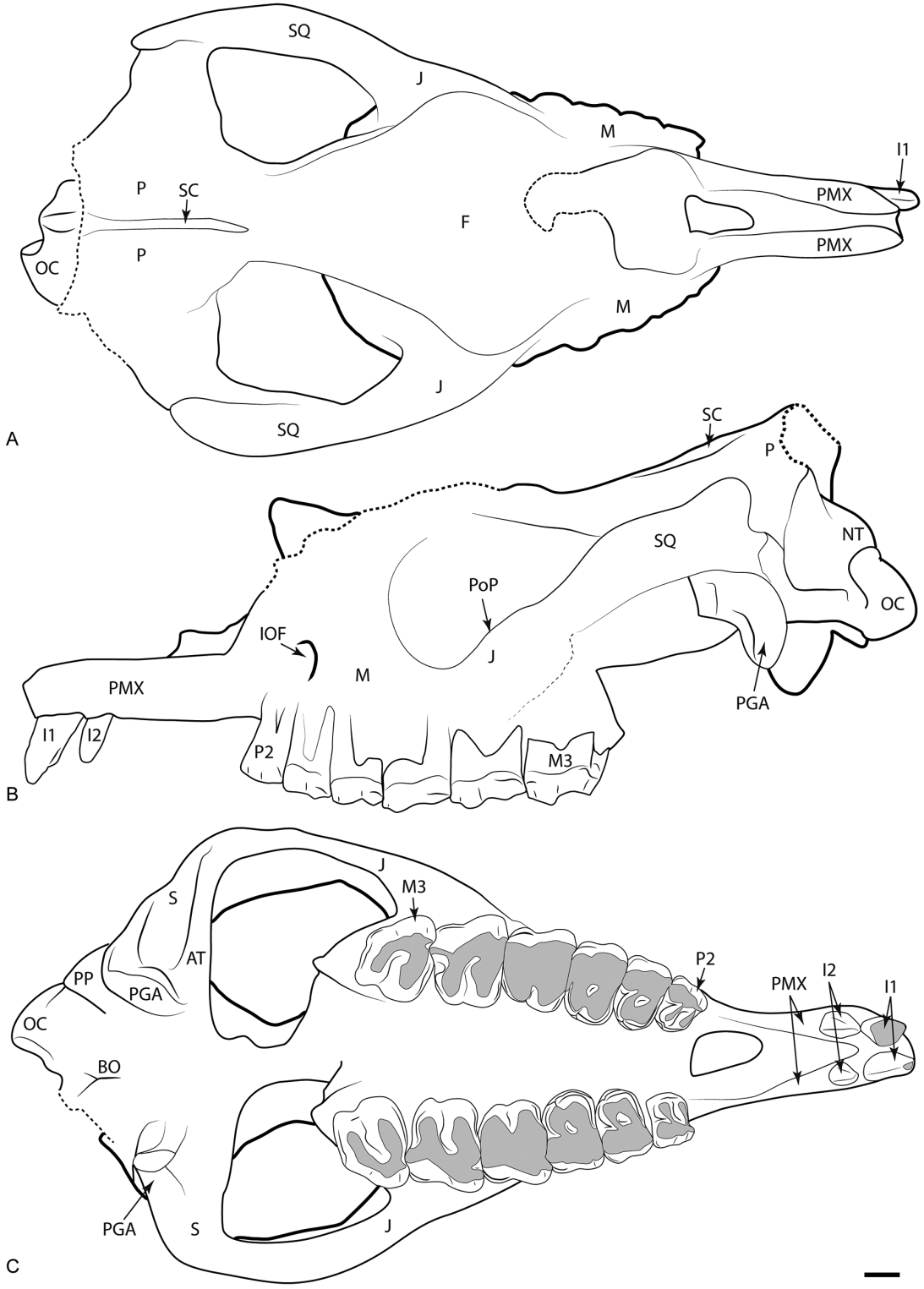

Fig. 23. *Ronzotherium heissigi* sp. nov. from Vendèze (late early Oligocene, France). Drawing of the skull MNHN.F.LIM181. **A**. Dorsal view. **B**. Left lateral view. **C**. Ventral view. Abbreviations: AT = articular tubercle; BO = basioccipital; F = frontal; IOF = infraorbital foramen; J = jugal; M = maxilla; NT = nuchal tubercle; OC = occipital condyle; P = parietal; PGA = postglenoid apophysis; PMX = premaxilla; PoP = postorbital process; PP = paraoccipital process; SC = sagittal crest; SQ = squamosal. Scale bar: 2 cm.

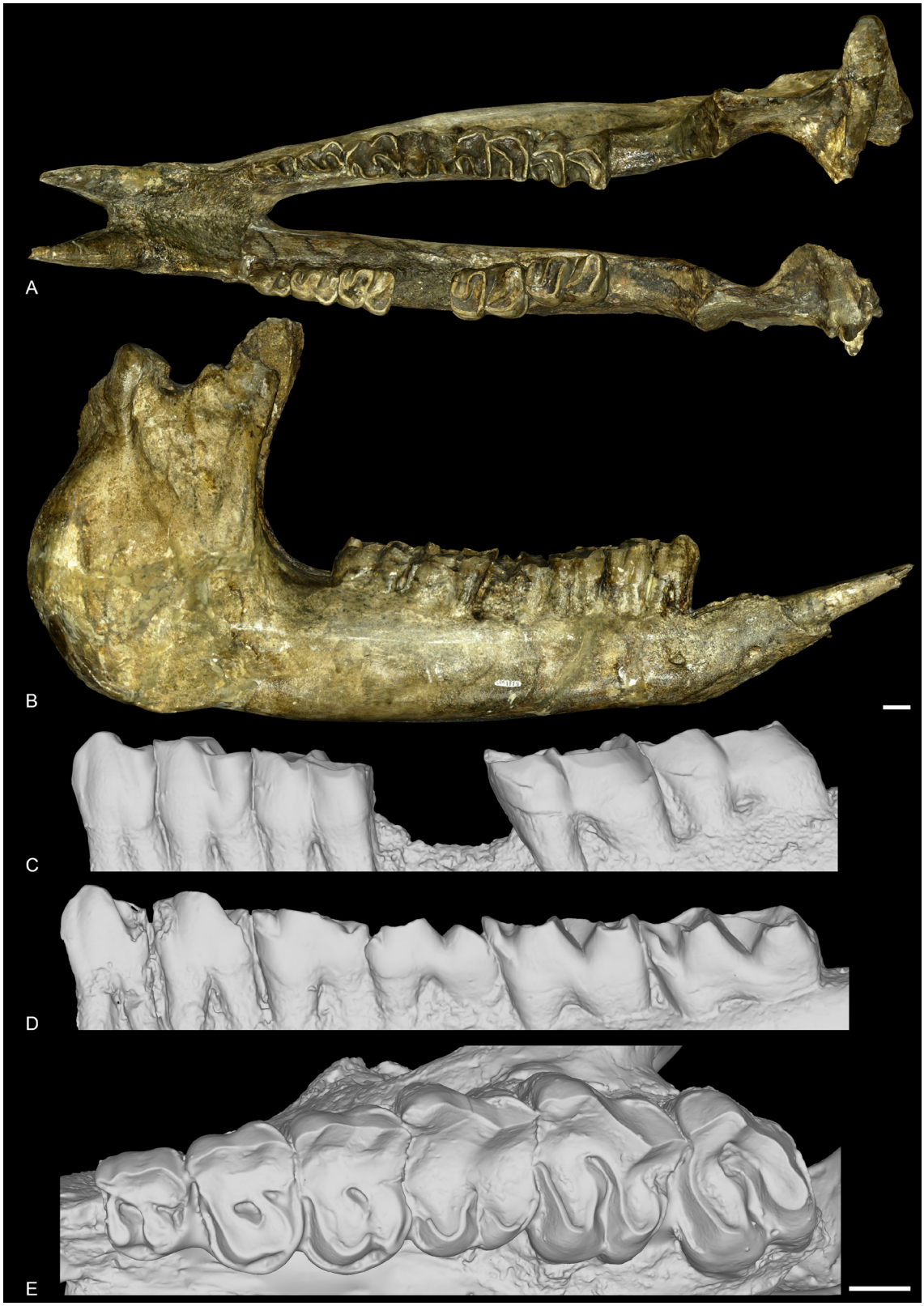

Fig. 24. *Ronzotherium* heissigi sp. nov. from Vendèze (late early Oligocene, France). **A–D**. Mandible MNHN.F.LIM181. **A**. Occlusal view. **B**. Lateral view. **C**. With left p2–p4 and m2–3 in labial view. View. **D**. Right p2–m3 in lingual view. – **E**. Skull MNHN.F.LIM181, belonging to the same individual as the mandible, close-up view of P2–M3 in occlusal view. Scale bars: 2 cm.

border of the corpus. The ventral base of the corpus is completely straight. The ramus is inclined forward in lateral view, and the coronoid process is well developed. In medial view, the foramen mandibulare is located below the teeth neck.

Dentition. The complete dental formula is I1–2, P2–M3 / i2, p2–m3. The Length(P3–4)/Length(M1–3) ratio is between 0.42 and 0.5. The cement is absent and the crowns are very low (Figs 22–24).

I1 is oval in cross-section, pointed and not chisel-shaped. It is directed downwards, and it bears two crests, one anterior and one posterior. There was no contact with the lower incisor (no visible wear on any of them). It is separated from I2 by a very short diastema. I2 overall has the same shape as I1 but is smaller and less pointed. The diastema between I2 and P2 is very long. The i1 is absent, and the space between the two i2 is very short. The i2 are large, tusk-shaped and parallel.

The labial cingulum of the upper premolars is always present, posteriorly, below the metastyle. The lingual one is always present, continuous and undulating in lingual view: it is high below the protocone, very low at the level of the median valley, and very high at the level of the hypocone. The crochet is always absent. The hypocone is connected to the ectoloph. The postfossette is narrow and the antecrochet is always absent. The P1 is absent. The protocone and hypocone of P2 are separated and the hypocone is posterior to the metacone. The metacone fold is strong. The protocone is same sized as the hypocone. The protoloph of P2 is joined to the ectoloph. The medifossette is always absent on the premolars and the protocone is never constricted. On P3–4, the protocone and hypocone are connected by a lingual wall. The metacone fold is strong. The hypocone is posterior to the metacone as on P2. The protoloph of P3 is joined to the ectoloph and the crista and pseudometaloph are absent. The antecrochet is always absent on P3–4. The metaloph of P4 is continuous.

The labial cingulum of the upper molars is always present, as on the premolars, below the metastyle. The antecrochet is present on M2, absent on M3 and not visible on M1. The crochet, crista, cristella and medifossette are always absent. The lingual cingulum is always absent. The protocone is never constricted. The paracone fold is strong and the metacone fold absent. The metastyle is long, but the parastyle is rather short. The metaloph is long. The posterior part of the ectoloph is straight. The posterior cingulum is continuous. There is no lingual groove on the protocone of M2 and the mesostyle is absent. The antecrochet and hypocone are well separated. The ectoloph and metaloph of M3 are fused into an ectometaloph, and it is quadrangular. The protocone is not constricted and the protoloph is transverse. The posterior groove of the ectometaloph is present.

The lower p2–3 do not bear vertical external rugosities. The external groove of the lower cheek teeth is angular and is developed until the neck. The trigonid is angular and forms an acute dihedron. The metaconid and entoconid are always joined to the hypolophid. The lingual opening of the lower premolars is V-shaped. The lingual cingulum is always absent on all lower cheek teeth and the labial one is basically absent, except anteriorly below the paralophid. The d/p1 is always absent. The paralophid of p2 is curved, without constriction and the paraconid is quite reduced. The posterior valley is lingually open. The lingual branch of the paralophid of p3 is long and developed. The anterolingual cingulum does not reach the metaconid. The hypolophid of the lower molar is transverse and there is no lingual groove of the entoconid.

Fig. 25 (next page). *Ronzotherium heissigi* sp. nov. from Bumbach, Bern Canton (early late Oligocene; Switzerland). – **A–D**. Mandible NMB-UM-6132. **A**. Occlusal view. **B**. Left lateral view. **C**. With right p3–m3 in labial view. **D**. With right p3–m3 in lingual view. – **E–F**. Right humerus NMB-UM-129a. **E**. Anterior view. **F**. Posterior view. – **G–H**. Left humerus NMB-UM-132. **G**. Anterior view. **H**. Posterior view. – **I–J**. Right radius NMB-UM-127a. **I**. Anterior view. **J**. Posterior view. – **K–M**. Right ulna NMB-UM-131b. **K**. Anterior view. **L**. Posterior view. **M**. Distal view. Abbreviation: im = insertion for the m. biceps brachii. Scale bars: 2 cm.

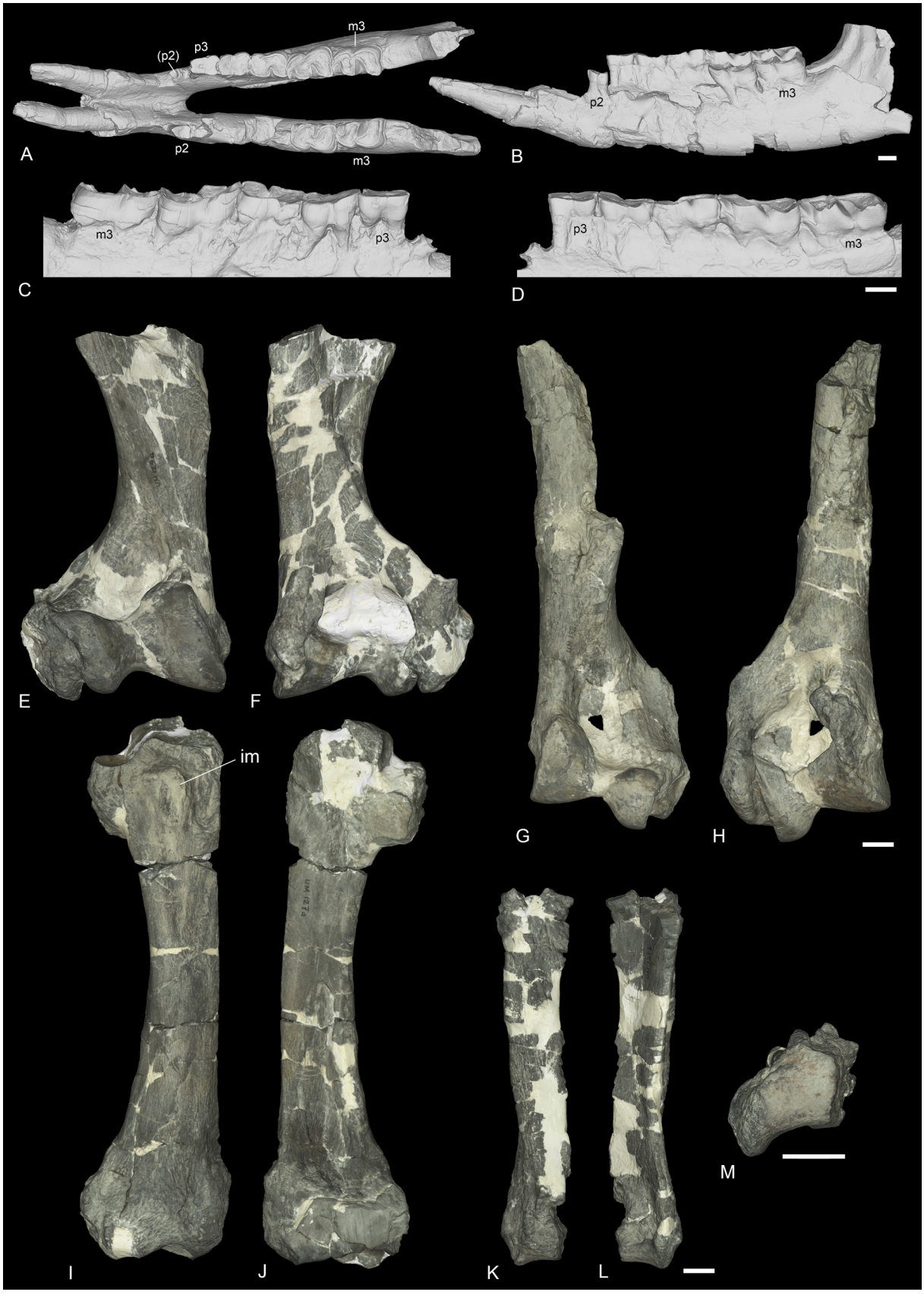
m3
(p2)
p3
p2
m3
A
p2
m3
B
m3
p3
C
p3
m3
D
E
F
im
G
H
I
J
K
L
M

Material from Bumbach

Newly prepared specimens are referred to as *Ronzotherium heissigi* sp. nov. and they document the only known postcranial remains of this species.

Humerus. The two humeri from Bumbach are proximally broken (Fig. 25E–H). In posterior view, the fossa olecrani is high on NMB-UM-132, but lower on the other humerus, NMB-UM-6132, possibly due to taphonomical deformation. The lateral epicondyle is very prominent, and distally elongated. The distal articulation is hourglass-shaped in anterior view, with a deep proximal incision between the two lips of the trochlea and the articulation is oblique. The epicondylar crest is high. The distal gutter on the epicondyle is strong in posterior view.

Radius. The radius from Bumbach (NMB-UM-127a, Fig. 25I–J) belongs to the same individual as the humerus NMB-UM-132. The anterior border of the proximal articulation is straight. The medial border of the diaphysis is straight. The insertion of the m. biceps brachii is deep and the gutter for the m. extensor carpi is deep and wide. The posterior expansion of the scaphoid facet is high and there is no secondary distal articulation for the ulna.

Ulna. The ulna NMB-UM-131b-c (Fig. 25K–M) belongs to the same individual as the radius (NMB-UM-127a) and the humerus (NMB-UM-132). It is very poorly preserved. The olecranon of the ulna is rather long and makes an open angle with the diaphysis. The distal end is large, the anterior tubercle and the lunate facet are absent, and the pyramidal facet is concave.

Lunate. The lunate NMBE-5035833 is complete and very well preserved (Fig. 26A–E). The proximal articulation for the radius is very large and convex anteroposteriorly. There is no articulation with the ulna. In proximal view, there is a long drop-like posterior extension of the radius facet on the medial side. The anterior side is deeply keeled, and the distal border is acute in anterior view. Medially, the two proximal articulations for the scaphoid are fused in a single facet. It is separated from the distal scaphoid facet by a deep groove. The distal facet for the scaphoid is large. In lateral view, the proximal and distal articulations for the pyramidal are large and the proximal one is medially displaced. In distal view, there are three articulation facets: a large anterior one for the unciform, and two for the magnum, one of which is distal and very concave and the other thin, flat and elongated is anterior, and located between the scaphoid and unciform facets.

Trapezoid. Two trapezoids are preserved from Bumbach (NMB-UM-6 and NMB-UM-6136b, Fig. 26F–J). The latter is slightly different from the former, and it articulates with the magnum NMB-UM-6136c and the McII NMB-UM-6136a. In anterior view, they are both wider than high. The proximal border is sigmoid on NMB-UM-6136b, whereas it is symmetric on NMB-UM-6. The magnum facet occupies most of the lateral side, while the medial side is occupied by the medio-distal articulation

Fig. 26 (next page). *Ronzotherium heissigi* sp. nov. from Bumbach, Bern Canton (early late Oligocene; Switzerland). – **A–E**. Left lunate NMBE-5035833. **A**. Anterior view. **B**. Proximal view. **C**. Distal view. **D**. Lateral view. **E**. Medial view. – **F–J**. Right trapezoid NMB-UM-6136b. **F**. Anterior view. **G**. Lateral view. **H**. Medial view. **I**. Proximal view. **J**. Distal view. – **K–N**. Right magnum NMB-UM-6136c. **K**. Anterior view. **L**. Distal view. **M**. Lateral view. **N**. Medial view. – **O–Q**. Right McII NMB-UM-121. **O**. Anterior view. **P**. Lateral view. **Q**. Proximal view. – **R–T**. Right McII NMB-UM-6136a. **R**. Proximal view. **S**. Anterior view. **T**. Lateral view. – **U–Y**. Right cuboid NMBE-5035834. **U**. Anterior view. **V**. Proximal view. **W**. Distal view. **X**. Medial view. **Y**. Lateral view. Abbreviations: a = astragalus; ca = calcaneus; e = ectocuneiform; l = lunate; m = magnum; n = navicular; p = pyramidal; r = radius; s = scaphoid; td = trapezoid; tm = trapezium; un = unciform. Scale bar: 2 cm.

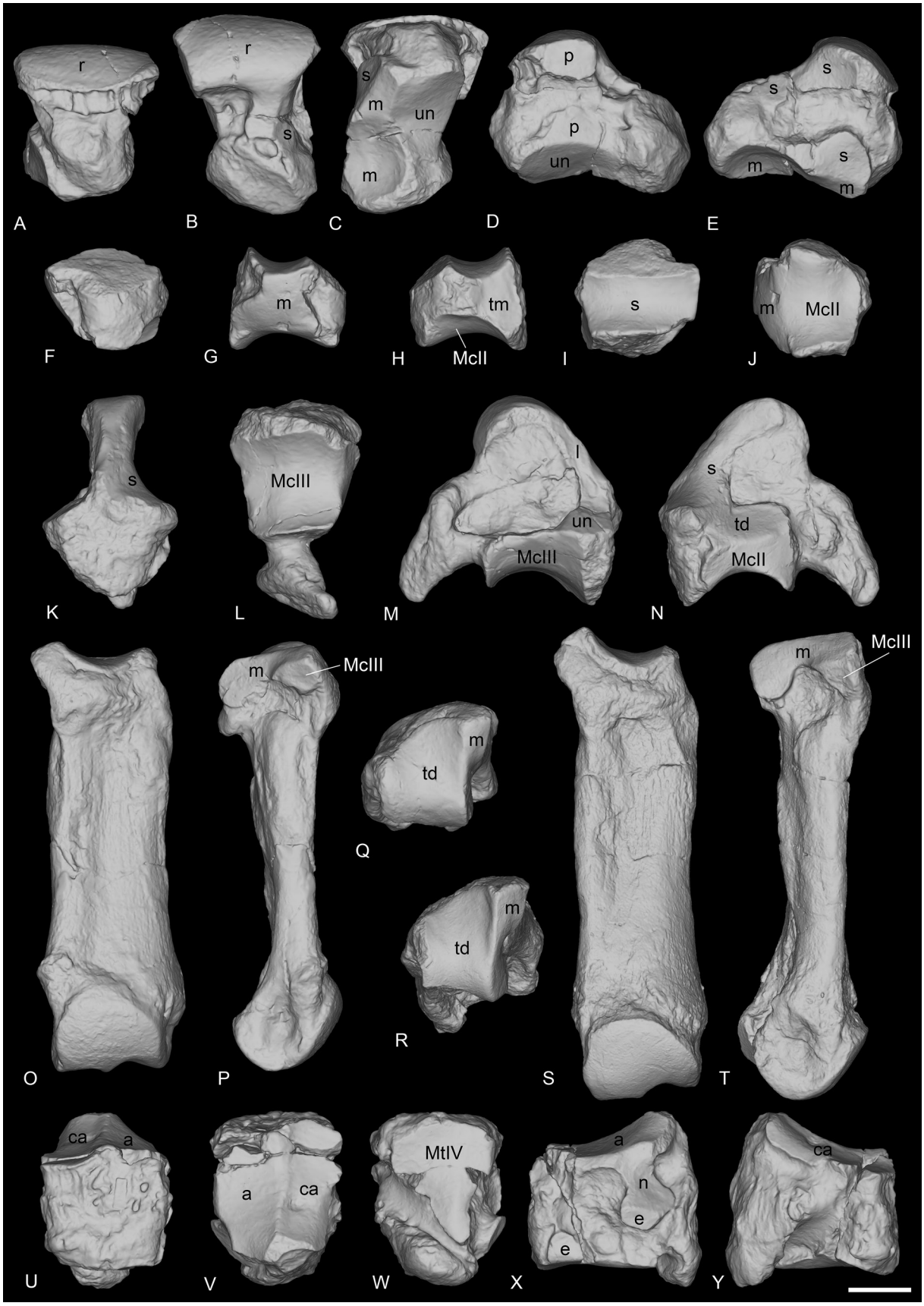
A
r
B
r
s
C
s
m
un
m
D
p
p
un
E
s
s
m
s
m
F
G
m
H
tm
McII
I
s
J
m
McII
K
s
L
McIII
M
l
un
McIII
N
s
td
McII
O
P
m
McIII
Q
m
td
R
m
td
S
T
m
McIII
U
ca
a
V
a
ca
W
MtIV
X
a
n
e
e
Y
ca

for the trapezium. The proximal side is fully occupied by the anteroposteriorly concave scaphoid facet. The distal articulation for the McII is also anteroposteriorly concave.

Magnum. The magnum NMB-UM-6136c is complete (Fig. 26K–N). In anterior view, the proximal border of the anterior side is concave and the anterior face is wider than high. The proximal apophysis is very high, very convex and narrow. The lunate facet on this apophysis is very long and contacts the small unciform facet. On the other side of the proximal apophysis, the facet for the scaphoid is also long and is very poorly distinguished from the medial facet for the trapezoid. This latter facet is longer than high. The medio-distal McII facet is flat and its distal border is very concave in medial view. On the distal side, the McIII facet is very large, quadrate, as long as wide and very concave anteroposteriorly. The posterior tuberosity of the magnum is short and curved.

McII. There are two McII preserved from Bumbach (NMB-UM-121 and McII NMB-6136a, Fig. 26R–T). The outline of the proximal side is trapezoidal. The articulation for the trapezoid is concave lateromedially and slightly convex anteroposteriorly. On the lateral side, the magnum facet is curved and band-shaped. The anterior facet for the McIII is present but the posterior is absent. There is no trapezium facet. The insertion for the m. extensor carpalis is salient.

Femur. Only a proximal fragment is preserved in Bumbach (NMBE-5035835). The head is hemispheric and the fovea capitis is high and narrow. The major trochanter is lower than the head and separated from it by a short neck. It is nearly triangular in proximal view and in lateral view the posterior part is higher than the anterior. The trochanteric fossa is deep on the posterior side, with a well-marked intertrochanteric crest. A fossa is also present on the anterior side, overhung by the major trochanter.

Cuboid. The cuboid NMBE-5035834 is complete (Fig. 26U–Y). The anterior side is approximately as high as wide. In lateral view, the posterior side is higher than the anterior and the posterior apophysis of the cuboid is slightly lower than the distal articulation. In proximal view, the posterior apophysis is almost not visible. The proximal side is oval and the astragalus and calcaneal facets are almost equal-sized. On the medial side, the postero-proximal and elongated facet for the navicular is concave and contacts the small, square and postero-mesial facet for the ectocuneiform. The navicular facet bears a thin extension up to the anterior border, bordering the astragalus facet. The small anterodistal facet for the ectocuneiform is separated from the posterior one by a wide groove. On the lateral side, the groove for the tendon of the m. fibularis longus is very large and deep. The distal articulation for the MtIV is flat and triangular.

Discussion

An exhaustive list of occurrences is given in Supp. file 4. These occurrences are represented on palaeogeographical reconstructions of Europe (Fig. 27), from the earliest Oligocene (MP21) to the latest Oligocene (MP30).

Body mass evolution

The body masses of specimens of *Ronzotherium* have been estimated based on the regression equations provided by Fortelius & Kappelman (1993) for Rhinocerotidae (Supp. file 5). These equations allow estimations based on different measurement from the skull, upper dentition, humerus, radius, femur and tibia. We also used equations provided by Tsubamoto (2014) to estimate the body mass based on measurements on the astragalus. The results show a very large variation, even based on a single bone, especially for the astragalus, which ranges from approximately 400 kg to 1100 kg for the astragalus PUY.2004.6.1770.RON, for example. However, one equation does not necessarily always give higher or lower estimations than another. For example, on the tibia 1970-158 from Villebramar, the T2 estimator (tibia proximal width) gives a smaller estimate than the T5 (tibia distal anteroposterior diameter)

(740 kg vs 1060 kg, respectively), whereas on the tibia 1973-221, it is the T5 estimator that gives a smaller estimate than the T2 (840 kg vs 1300 kg, respectively). These differences are probably due to deformations or bad preservations of specimens. Thus, these estimated body masses should be taken with a lot of caution, and they probably do not reflect a realistic body mass for these animals. Yet, they can provide a base for comparisons, since equivalent equations are used for all specimens.

The average body mass for each population is represented in Fig. 27 and is placed on palaeogeographical maps. From this figure, we clearly observe the very large intraspecific and interspecific variation of the estimated body mass of *Ronzotherium*, and no clear trend through time can be detected. However, all

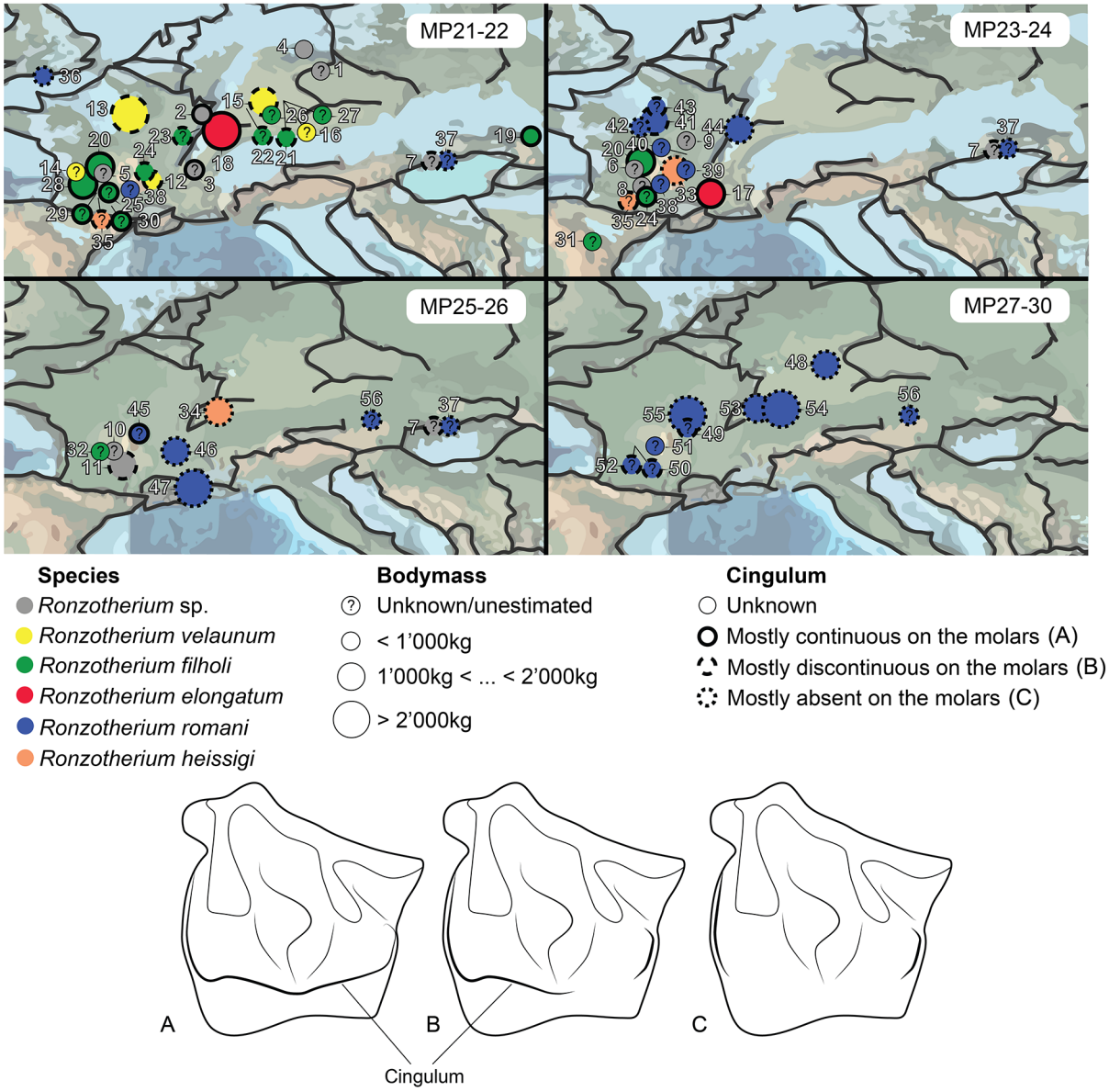

Fig. 27. Occurrences of *Ronzotherium* Aymard, 1854 in Europe, from MP21 (earliest Oligocene) to MP30 (latest Oligocene) with palaeogeographical reconstructions, modified from PALEOMAP (Scotese 2016). The diameter of the circles is proportional to the body mass of the specimens in each locality, and the thickness and shape of the outline refer to the shape of their cingulum. Numbers of circles refer to the number of the locality in Supp. file 4.

body masses below 1000 kg are found during the early Oligocene, with *Ronzotherium velaunum* in Ronzon (n° 11), *R.* cf. *romani* in Bouldnor (n° 35), *R.* sp. in Pechelbronn (n° 2) and Espenhain (n° 3) and *R. filholi* in Cluj-Napoca (n° 18), Möhren (n° 20) and Bournoncle (n° 23). *Ronzotherium velaunum* shows the highest variation of body mass, ranging from less than 1000 kg in Ronzon (n° 11), to more than 2000 kg in Lagny-Thorigny (n° 12). However, for this latter locality, only one estimator could be used to estimate its body mass (length of M2) and should thus be taken with even more caution. Finally, there does not seem to be any obvious correlation between the strength of the cingulum and the body mass, since large masses are found in species having complete cingulum (*R. elongatum*) as well as those having extremely reduced cingulum (*R. romani*).

Cingulum

Interestingly, the shape, strength and size of the cingulum of the cheek teeth seem to follow a trend of reduction through time. Furthermore, *Ronzotherium romani* and *R. heissigi* sp. nov. are the two species

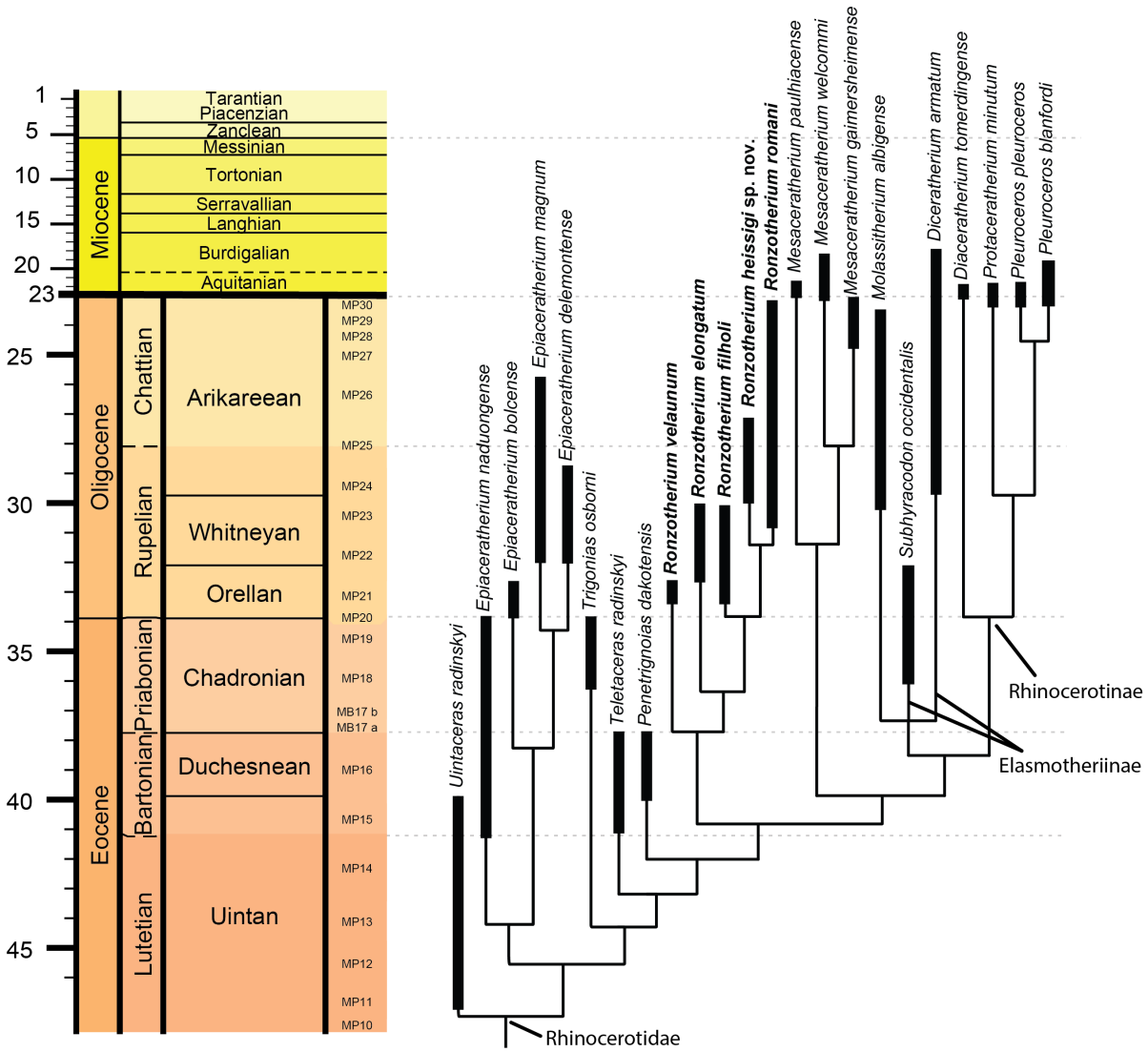

Fig. 28. Cladogram of Rhinocerotidae Owen, 1845 calibrated in time. Bold lines indicate the temporal range of each terminal. Temporal scale for the Miocene and younger periods has been compressed and differs from the Eocene and Oligocene.

that show the most discontinuous cingulum while *R. romani* is the only one that survived until the end of the Oligocene (Fig. 28).

It was first suggested that the biological role of the cingulum was to provide protection to the gums and the periodontal membrane (Mills 1967), but Lucas *et al*. (2008) recently proposed another hypothesis. According to them, and after testing their hypothesis with finite elements analyses, the cingulum could also protect from enamel cracks or fractures, by strengthening the crown base, especially during the mastication of soft food. More recently, Anderson *et al*. (2011) further tested this hypothesis by controlling the influence of several factors (hard vs soft food, symmetrical vs asymmetrical loads, size and shape of cingulum, etc.), and showed that, most of the time, having a cingulum could indeed protect from enamel fractures caused by mastication. Based on their results, having a complete cingulum (i.e., which surrounds the whole neck of the tooth) is only efficient if it is formed by actually creating more enamel around the tooth, which leads to additional enamel surface and volume. However, this hypothesis supposes that the generation of this additional enamel would be more costly during the development of the tooth, which could thus imply a trade-off. Yet, having even just a partial cingulum (i.e., a cingulum which is interrupted lingually or labially, for example) is almost as efficient as having a complete cingulum under a soft load (15 % crack reduction vs 18 % reduction with complete standard cingulum; see Anderson *et al*. 2011: table 1), but is also less costly. Furthermore, if the cingulum is not generated by adding enamel, but by restructuring the shape of the crown enamel (i.e., no additional enamel is needed for the formation of this cingulum, and thus no additional cost), then having a complete cingulum leads in fact to more fractures than without a cingulum, whereas having a partial cingulum still slightly reduces the number of fractures. Thus, considering the possible trade-off related to the developmental cost of the cingulum, and considering that complete cingulum is actually inefficient if it is not actually adding enamel surface, it would seem credible that the individuals of *Ronzotherium* having partial cingulum had been naturally selected and survived longer than the individuals having a complete cingulum. Perhaps this could explain the reduction trend observed in the cingulum size in this genus, though it would need further quantitative investigation. If this hypothesis were validated, it could partially explain the early disappearance of most species of *Ronzotherium*, while only *R. romani*, which has the most reduced cingulum, would have passed natural selection.

Conclusion

Ronzotherium is the most characteristic rhinocerotid from the Oligocene of Europe. Appearing from the earliest Oligocene and lasting to the latest Oligocene, it also had the longest timespan of all the European Oligocene Rhinocerotidae. Yet, and even though it was quite commonly found at numerous European localities, it remained under-investigated and its phylogeny had never been elucidated. This absence of well-defined systematics for this taxon had led to several contradictions in its taxonomy, which we hope are now partly enlightened. Five species can be distinguished and characterised, including a new species: *Ronzotherium heissigi* sp. nov. The postcranial skeleton of *Ronzotherium romani*, which was very poorly known, is now identified and described from several localities for the first time. A comprehensive map of the distribution of *Ronzotherium* is proposed and shows that only *R. romani* remained during the latest Oligocene. We finally discussed the evolution of the body mass and cingulum of this genus through time and suggest that the long survival of *R. romani* may have been linked to the reduction of the cingulum.

Acknowledgements

We are extremely grateful to all curators and collection managers who helped and allowed us to study the specimens presented here: Gertrud Rößner and Kurt Heissig (BSPG), Vlad Codrea (MBT), Astrid Bonnet and Emmanuel Magne (PUY), Robin Marchant (MGL), Patrice Blain, Pascal Girodon and Anne-Laure Boukef (MHNB41), Christophe Borrely (MHNM), Yves Laurent (TLM), Christine Argot, Guillaume